

## Estimating uncertainty in limit state capacities for reinforced concrete frame structures through pushover analysis

Xiaohui Yu<sup>1a</sup>, Dagang Lu<sup>1b</sup> and Bing Li<sup>2\*</sup>

<sup>1</sup>Ministry-of-Education Key Lab of Structures Dynamic Behavior and Control, School of Civil Engineering, Harbin Institute of Technology, Harbin 150090, China

<sup>2</sup>School of Civil and Environmental Engineering, Nanyang Technological University, 639798, Singapore

(Received October 18, 2014, Revised October 27, 2015, Accepted November 12, 2015)

**Abstract.** In seismic fragility and risk analysis, the definition of structural limit state (LS) capacities is of crucial importance. Traditionally, LS capacities are defined according to design code provisions or using deterministic pushover analysis without considering the inherent randomness of structural parameters. To assess the effects of structural randomness on LS capacities, ten structural parameters that include material strengths and gravity loads are considered as random variables, and a probabilistic pushover method based on a correlation-controlled Latin hypercube sampling technique is used to estimate the uncertainties in LS capacities for four typical reinforced concrete frame buildings. A series of ten LSs are identified from the pushover curves based on the design-code-given thresholds and the available damage-controlled criteria. The obtained LS capacities are further represented by a lognormal model with the median  $m_C$  and the dispersion  $\beta_C$ . The results show that structural uncertainties have limited influence on  $m_C$  for the LSs other than that near collapse. The commonly used assumption of  $\beta_C$  between 0.25 and 0.30 overestimates the uncertainties in LS capacities for each individual building, but they are suitable for a building group with moderate damages. A low uncertainty as  $\beta_C=0.1\sim 0.15$  is adequate for the LSs associated with slight damages of structures, while a large uncertainty as  $\beta_C=0.40\sim 0.45$  is suggested for the LSs near collapse.

**Keywords:** limit state; pushover analysis; RC frame; uncertainty analysis; correlation-reduced Latin hypercube sampling

### 1. Introduction

Reinforced concrete (RC) frames are commonly found around the world and are often subjected to substantial damage during earthquakes. Considering the uncertain nature of earthquakes and structural parameters, probabilistic approaches such as the fragility curves and the probabilistic risk analysis tools are usually used to estimate the seismic safety of the RC frames.

In these probabilistic methods, it is crucial to obtain a rational and quantitative definition of the structural limit state (LS) capacity (Favvata *et al.* 2014, Zhang and Goh 2014). In fact, different

---

\*Corresponding author, Associate Professor, E-mail: CBLi@ntu.edu.sg

<sup>a</sup>Assistant Professor, E-mail: xiaohui.yu@hit.edu.cn

<sup>b</sup>Professor, E-mail: ludagang@hit.edu.cn

seismic design codes have provided various empirical thresholds to define the LSs for RC frame structures. For instance, the US standard, “*Seismic Rehabilitation of Existing Buildings*” (ASCE/SEI 41-06 2007), defines three performance LSs, namely, Immediate Occupancy (IO), Life Safety (LS) and Collapse Prevention (CP), by the drift limits of 1%, 2% and 4%, respectively. In the current version of the Chinese code, *National Standard of the People’s Republic of China, Code for Seismic Design of Building* (GB50011 2010), two drift thresholds of 0.18% (1/550) and 2% (1/50) are recommended to identify the LSs that are labeled as elastic limit and plastic limit, respectively. The above code-provided thresholds are generated based on experiment data, aftershock investigations and expert judgments and therefore they are empirical models that tend to be conservative. As noted in ASCE/SEI 41-06 (2007), the code-provided drift limits are only indicative of the range of displacement that the typical structure may undergo in response to various loads at different performance levels. From another aspect, the code-provided thresholds can only be treated as the general guidelines rather than the strict criteria to judge the LS capacities for a particular building against earthquake-induced damages.

To deal with the above limitations, experiments may be the best way to assess the real capacity of the concerned building by observing its damages under earthquakes. This method has been used to determine the LS capacities for RC elements (Gardoni *et al.* 2002, Choe *et al.* 2007, Tran and Li 2013, 2015); however it is limited for building systems in terms of applicability and a simulation-based method represents a more feasible alternative. The pushover curve, also viewed as the capacity curve (ATC40 1996; FEMA 1999), can better capture the realistic performance for a given building and is widely used for seismic fragility analysis (Wen *et al.* 2004, Erberik and Elnashai 2004, Kwon and Elnashai 2006, Ji *et al.* 2007, Pasticier *et al.* 2008, Erberik 2008, Shome and Paolo 2010, Rota *et al.* 2010, Ozel and Guneyisi 2011, Mwafy 2012, Frankie *et al.* 2013). However, it is not an easy task to determine the LSs of interest on a pushover curve because there have been no widely accepted criteria because of different understandings of structural damage behaviors. This means that code-provided thresholds rather than the pushover-based results still represent the convention today (Ramamoorthy *et al.* 2006, Hueste and Bai 2007, Ellingwood *et al.* 2007, Celik and Ellingwood 2010). However, this does not detract from the fact that defining LS capacities on a pushover curve remains an important and viable step going forward.

The LS capacities of structures are highly dependent on the characteristics of structures such as material strengths, element geometries and gravity loads, etc. These characteristics are inherent random and thus lead to considerable uncertainty in the LS capacities. It is therefore reasonable to describe LS capacities with a probabilistic model rather than a deterministic one. According to the SAC/FEMA methodology (Cornell *et al.* 2002), lognormal distributions are commonly assumed for the concerned LSs with the parameters as the median capacity  $m_C$  and the logarithmic standard deviation (dispersion)  $\beta_C$ . Due to lack of real damage data,  $m_C$  was often assigned with the code-provided thresholds (Ramamoorthy *et al.* 2006, Ellingwood *et al.* 2007, Howary and Mehanny 2011) or identified from the deterministic pushover curve (Erberik and Elnashai 2004, Kwon and Elnashai 2006, Ji *et al.* 2007, Ramamoorthy *et al.* 2006), while  $\beta_C$  was commonly defined with an empirical value based on engineering experiences and judgments (Wen *et al.* 2004, Ramamoorthy *et al.* 2006, Hueste and Bai 2007, Ellingwood *et al.* 2007). However, such a simplistic treatment of  $m_C$  and  $\beta_C$  may not reflect the real probabilistic properties of the LS capacities and merits the further study.

The main goal of this study is not to define new LSs but to assess the uncertainties in LS capacities of RC frame buildings with focus on the effect of the variability of structural parameters. To this end, the conventional (deterministic) pushover analysis is extended based on a

correlation-controlled Latin hypercube sampling technique. A group of possible structural samples are generated for accounting for the randomness inherent the material strengths and gravity loads. A series of ten LSs using the code-provided thresholds and the available damage-controlled criteria are identified from the pushover curves and they are further represented by the lognormal distributions. The effects of the considered structural uncertainties on LS capacities are then assessed via the variation of  $m_C$  and  $\beta_C$ .

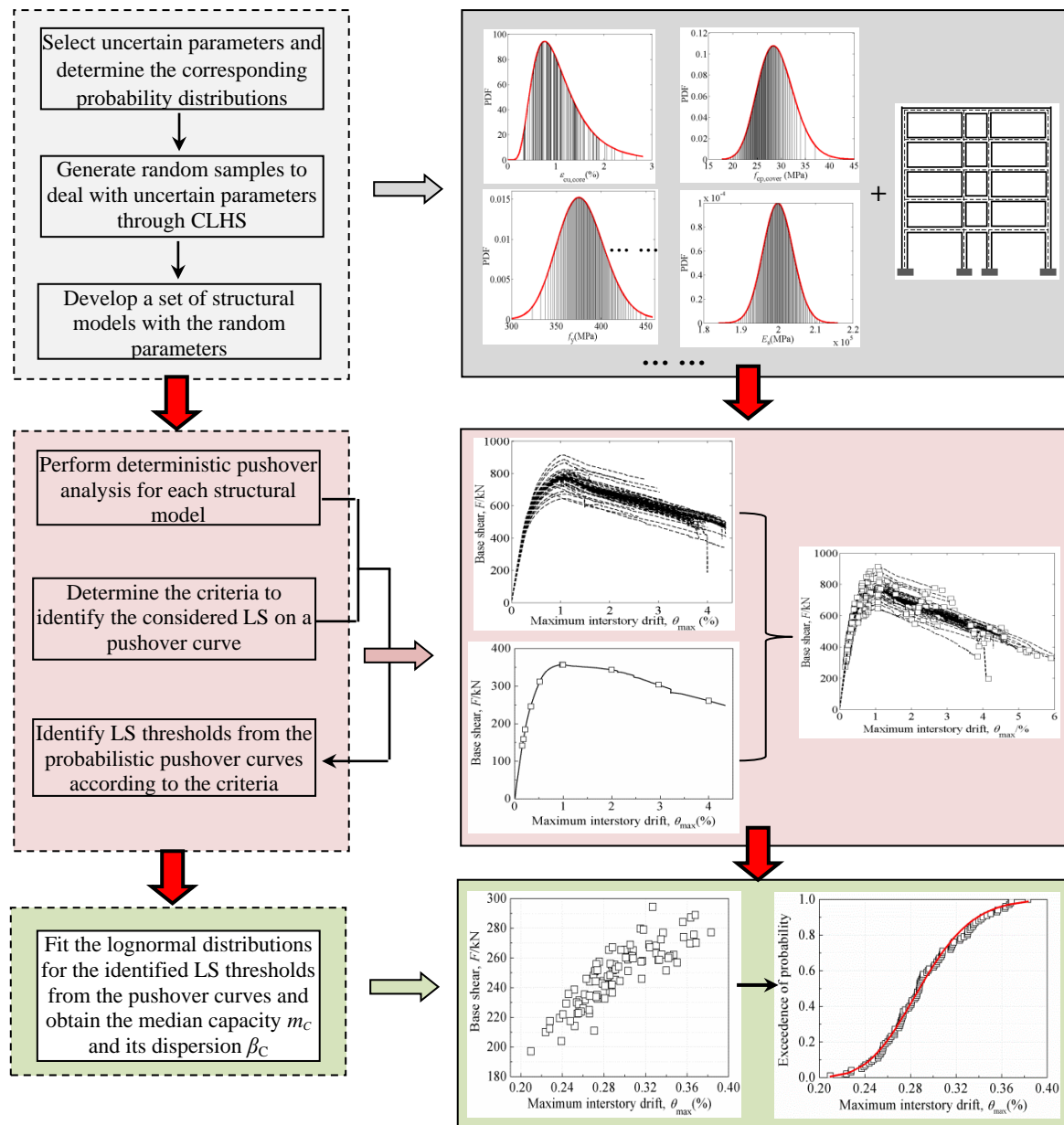


Fig. 1 Flowchart of the uncertainty study

## 2. Summary of the uncertainty study

The extended pushover procedure aims to consider the effects of the structural uncertainties on LS capacities. This goal is achieved by introducing a set of structural models, which reflect the structural uncertainty. These random structural models are used to generate probabilistic pushover curves. On the obtained pushover responses, the capacities of the considered LSs are identified and examined by statistics. Fig. 1 summarizes the analytical methodology of this study. Three main steps are involved, namely, the generation of structural models, the identification of the considered LSs on pushover curves, and the statistics of the acquired LS capacities. They are described in details in the following sections.

### 2.1 Generation of structural models

The primary task to generate the structural model set is to determine the uncertain parameters of structures. Ten structural parameters are considered as random variables, which will be described in Section 4. Once the probabilistic properties of the considered uncertain parameters are given, the random samples can be derived according to numerical simulation methods. The general Monte Carlo simulation (Tomos and Trezos 2006) and the First Order Second Moment method (FOSM) (Barbato *et al.* 2010) have been used in pushover analysis to account for structural uncertainties. Both methods have their pros and cons. The general Monte Carlo simulation is highly accurate but requires large computation efforts. FOSM greatly reduces the computation cost by calculating structural mean responses at the mean parameters but it may lead to inaccuracies in cases where the nonlinearity and uncertainty of structures cause a shift in the prediction of mean responses.

To balance these concerns, Monte Carlo simulation with the Latin hypercube sampling (LHS) technique has been widely adopted to examine the influences of structural uncertainties on seismic responses (Celik and Ellingwood 2010, Vamvatsikos and Fragiadakis 2010, Dolšek 2009, 2012). Nevertheless the standard LHS technique would introduce undesired spurious correlation into the samples. To overcome this shortcoming, a correlation-reduced LHS (CLHS) technique is employed in this study. For reasons of completeness, the main procedures of the CLHS for random sampling are briefly introduced hereafter, and the detailed mathematic backgrounds can refer to Olsson and Sandberg (2002).

The random samples are firstly generated by

$$\mathbf{x}_i = F_i^{-1} \left( \frac{\mathbf{P}_i - \mathbf{R}_i}{N_{\text{sam}}} \right), \quad i=1, \dots, N_{\text{var}} \quad (1)$$

where  $\mathbf{x}_i$  is the sample column of the variable  $X_i$ ;  $F_i^{-1}(\cdot)$  represents the inverse marginal cumulative distribution function of  $X_i$ ;  $\mathbf{R}_i$  is the random number element generated from the uniform (0,1) distribution;  $\mathbf{P}_i$  is the permutation of  $1, \dots, N_{\text{sam}}$ ; and  $N_{\text{var}}$  and  $N_{\text{sam}}$  are the numbers of uncertain parameters and random samples, respectively.

The elements of the permutation matrix  $\mathbf{P}$  are then divided by the number of realizations plus one, and mapped on the standard normal distribution by

$$\mathbf{y}_i = \Phi^{-1} \left( \frac{\mathbf{P}_i}{N_{\text{sam}} + 1} \right), \quad i=1, \dots, N_{\text{var}} \quad (2)$$

where  $\Phi^{-1}(\cdot)$  is the inverse standard normal distribution.

Through Cholesky decomposition, the correlation matrixes of  $\mathbf{Y}$  and  $\mathbf{X}$  are respectively decomposed as  $\mathbf{L}_0\mathbf{L}_0^T$  and  $\mathbf{L}_1\mathbf{L}_1^T$ , where  $\mathbf{L}_0$  and  $\mathbf{L}_1$  are both the lower-triangular matrixes. A new matrix  $\mathbf{Y}^*$  is consequently derived by

$$\mathbf{Y}^* = \mathbf{L}_1\mathbf{L}_0^{-1}\mathbf{Y} \tag{3}$$

The ranks of the columns of  $\mathbf{Y}^*$  (permutation of  $1, \dots, n$ ) become the corresponding elements in the columns of the matrix  $\mathbf{P}^*$ . Replace  $\mathbf{P}_i$  with  $\mathbf{P}_i^*$  and the random samples with reducing the unexpected spurious correlation are provided by Eq. (1).

One hundred random samples are generated to deal with the considered uncertain parameters. According to Olsson and Sandberg (2002), the CLHS with 100 samples can provide better results than the standard LHS involving 1000 samples. These generated random parameters are then assigned to the deterministic structural model and the structural model set is derived.

### 2.2 Identification of LS capacities on pushover curves

After generating the structural model set, pushover analyses are repeatedly performed for each model and a group of pushover curves in coordinates of base shear  $F$  and maximum inter-story drift angle  $\theta_{max}$  are generated. From these curves, two categories of criteria are considered to identify the LS capacities. The first category is based on the code-provided drift thresholds, where the  $F$  capacities conditioned on the limits of  $\theta_{max}=0.18\%$  (1/550), 1%, 2% (1/50) and 4% are acquired on a pushover curve for defining  $LS_1$ ,  $LS_2$ ,  $LS_3$  and  $LS_4$ , respectively (see Fig. 2(a)). For the cases where the pushover responses could not attain the drift of 4%, the ending of the pushover curve is used as an alternative (see Fig. 2(b)). Amongst these code-provided drift thresholds, the ones defined by 0.18% and 2% are adopted in GB50011-2010 (2010) for defining the performance limits in terms of elastic limit and plastic limit, respectively. The drifts of 1%, 2% and 4% are recommended in ASCE/SEI41-06 (2007) and widely used for defining the performance limits of IO, LS and CP, respectively.

As for the second category of criteria, six drift limits are captured from the pushover curves based on both the local- and global-level damages of structures, as shown in Fig. 3. In the local

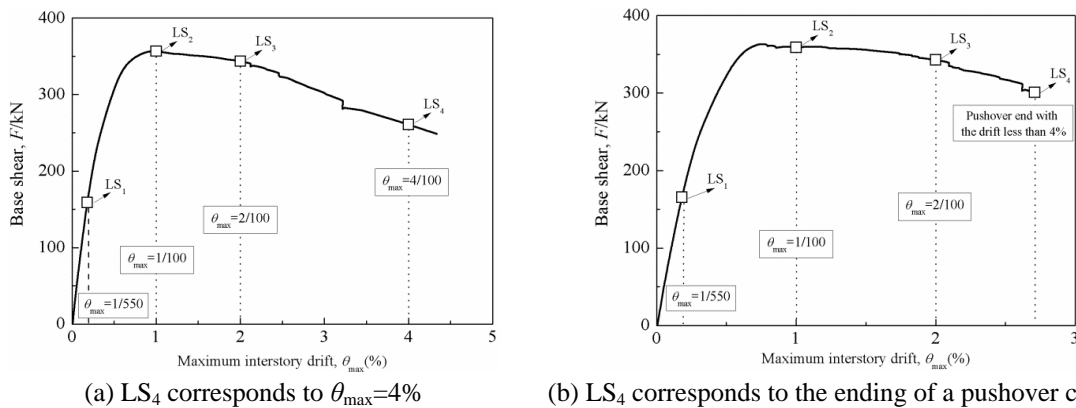


Fig. 2 The code-provide thresholds on a pushover curve

damage-based criteria, the element behaviors are monitored and mapped onto the global pushover curve once the prescribed damage limits are reached. In this study, the first appearance of concrete cracking and steel yielding on elements are taken as the local damage limits. The global damage-based criteria involve the global yielding point through idealizing the equivalent elastic-plastic system with the principle of equal energy absorption (Mwafy 2012, Frankie *et al.* 2013), the peak resistance (Tomos and Trezos 2006) and the 20% reduced post-peak capacity (Rota *et al.* 2010, Pasticier *et al.* 2008). There are two commonly used approaches to idealize the equivalent elastic-plastic system, which are the one recommended in ASCE/SEI41-6 (2007) (see Fig. 4(a)) and the other one proposed by Park (1988) (see Fig. 4(b)). They are both used here for defining the global yielding point.

The afore-mentioned two categories of LSs and the corresponding definition criteria are summarized in Table 1, where  $F$  is used as the capacity indicator for the first category of LSs

Table 1 The considered criteria to identify LS capacities on a pushover curve

Category	No.	Capacity indicator	Description
Code-provided thresholds	LS <sub>1</sub>	$F/kN$	$\theta_{max}=1/550=0.18\%$
	LS <sub>3</sub>		$\theta_{max}=1\%$
	LS <sub>3</sub>		$\theta_{max}=2\%$
	LS <sub>4</sub>		$\theta_{max}=4\%$
Damage-based criteria	LS <sub>5</sub>	$\theta_{max}/\%$	First crack presence in the elements of structures
	LS <sub>6</sub>		First yielding presence on the longitude reinforcement in the elements of structures
	LS <sub>7</sub>		Global yielding defined by the equivalent elasto-plastic system that is generated by ASCE method
	LS <sub>8</sub>		Global yielding defined by the equivalent elasto-plastic system that is generated by Park method
	LS <sub>9</sub>		Peak resistance
	LS <sub>10</sub>		20% reduced post-peak capacity

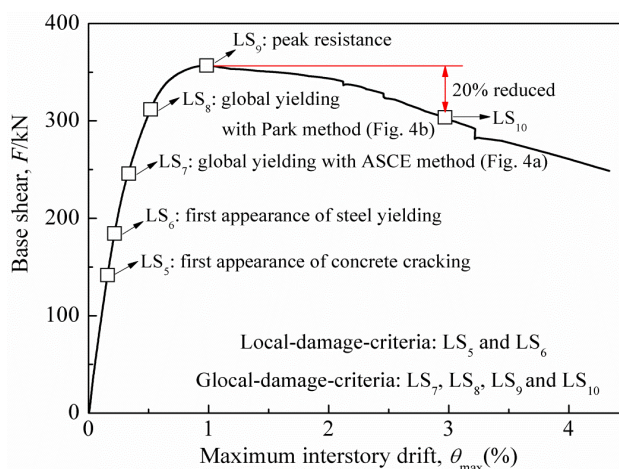


Fig. 3 Identification of LS thresholds based on the local and global damages

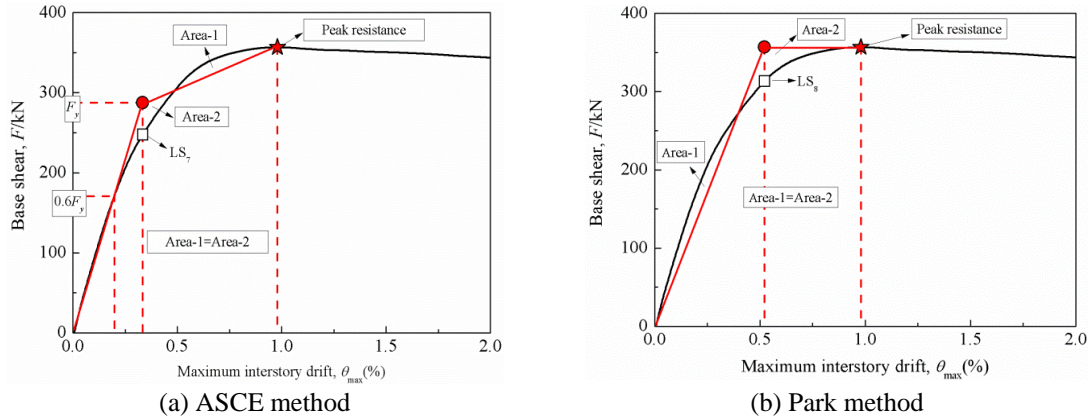


Fig. 4 Definition of the global yielding point based on ASCE method and Park method

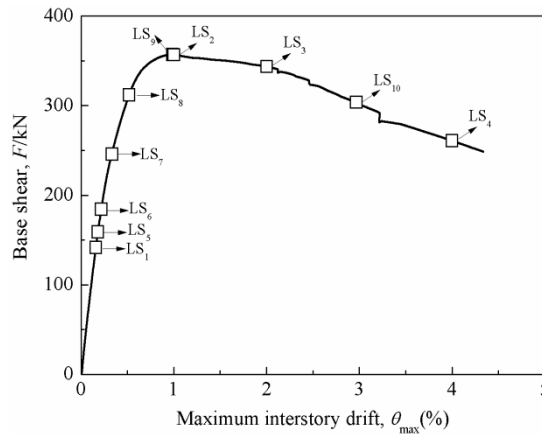


Fig. 5 Identification of the considered LSs on a pushover curve

( $LS_1 \sim LS_4$ ) based on the code-provided drift thresholds, while  $\theta_{max}$  is the capacity indicator for the second category of LSs ( $LS_5 \sim LS_{10}$ ) according to the specific structural damages. Note that there are still other special points that can be identified on the pushover curve to define the LS capacities according to different considerations. However this study does not aim to propose the optimum definition of LSs with pushover analysis but looks to examine the uncertainties in LS capacities. Fig. 5 demonstrates the considered LSs on a pushover curve. As seen from the figure the considered LSs have almost covered the entire damage process of the given structure and are therefore sufficient for this study.

### 2.3 Statistics of the acquired LS capacities

The obtained LS capacities from the pushover curves form the data pool for further statistics. The lognormal distributions for different LSs are fitted by the method of least squares. The derived distribution parameters as the median capacity  $m_C$  and the capacity dispersion  $\beta_C$  are examined to detract the effect of structural uncertainties on LS capacities. At first the fitted median capacity  $m_C$  is compared with the LS capacities determined from the deterministic structural model with

assigned median parameters. If there is a significant difference between them, the conventionally used code-provided and the deterministic pushover-based thresholds should be reconsidered as the assumption for  $m_C$ . As for the capacity dispersion  $\beta_C$ , the statistical values of  $\beta_C$  are compared with the widely used assumptions of  $\beta_C=0.3$  (Wen *et al.* 2004) and  $\beta_C=0.25$  (Ellingwood *et al.* 2007). This comparison could investigate the validation of these assumptions and help establish the quantitative perspective on the variation in LS capacities due to the uncertainties inherent structural characteristics.

### 3. Case study buildings

#### 3.1 Structural design

Four RC frame buildings with 3, 5, 8 and 10 stories were considered as the study cases. Fig. 6 provides the plan and elevation views of the case study buildings. It is noted that these buildings

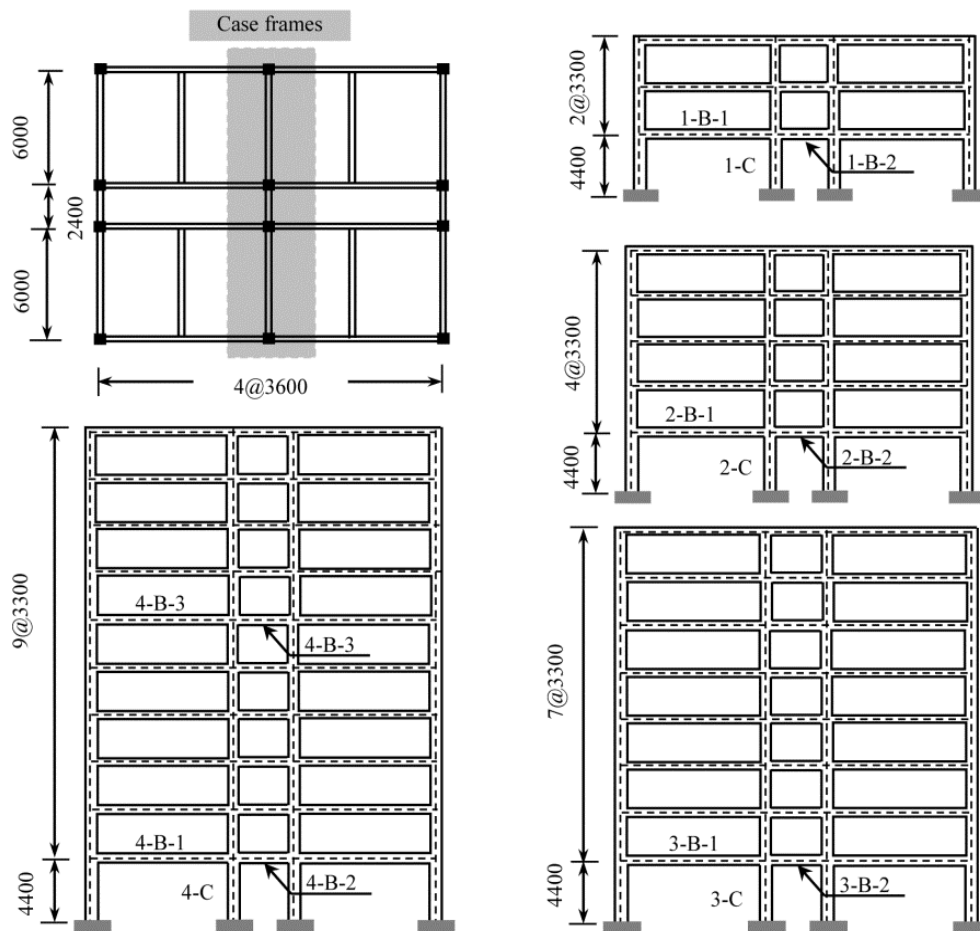


Fig. 6 Plan and elevation views of the example frames (unit: mm)

have the same plan arrangement, where a long corridor runs through the center of the floor plan parallel to the long direction of the building. This plan arrangement is very typical for low-to-mid-rise RC frame construction in China, and it creates frames in the transverse direction composed of longer exterior bays with a narrower interior bay.

The buildings were designed according to GB50011 (2010) with the design peak ground accelerations of 0.05 g, 0.10 g, 0.15 g and 0.20 g in correspondence to the 3-, 5-, 8- and 10-story buildings, respectively. All buildings were assumed to be founded on a medium stiff soil consisting of medium dense detritus, gravel or medium sand. This soil condition belongs to the site-class II with an equivalent shear wave velocity between 250-500 m/s (GB50011 2010). The design characteristic period of ground motion is 0.35 s. Earthquake loading was considered together with gravity loading  $G+0.5Q$ , where  $G$  denotes the permanent loads and  $Q$  represents the live loads. The permanent loads, including exterior walls, interior light partitions, and superimposed dead load, were assumed to be 4.5 kN/m<sup>2</sup>. The live load was assumed to be 2.0 kN/m<sup>2</sup> according to the requirement for civil buildings. The structural concrete members were designed according to the *Chinese Code for Design of Concrete Structures* (GB50010 2010). Fig. 7 gives the section dimensions and the reinforcement details for the typical columns and beams. For each building, a uniform section was used for the columns and two types of sections were designed for the beams of the longer exterior bays and that of the shorter interior bays. The nominal properties of the materials used in design are: 1) compressive strength of concrete is 26.8 MPa; 2) Young's modulus of concrete is 32500 MPa; 3) yield strengths of longitudinal and transverse reinforcement are 400 MPa and 235 MPa, respectively; and 4) Elastic modulus of reinforcement is 200 GPa (GB50010 2010).

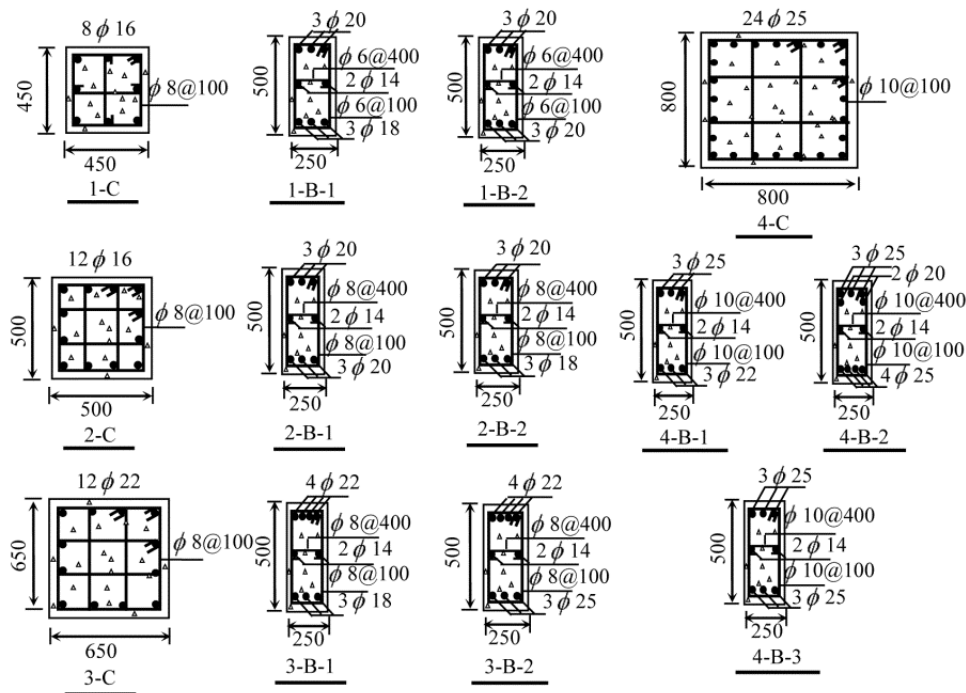


Fig.7 Reinforcing details of the typical beams and columns (unit: mm)

### 3.2 Structural model

The finite element (FE) structural analysis program OpenSees (2012) was utilized to develop analytical models and perform inelastic analysis for the case buildings. A two-dimensional FE model was used due to the symmetrical configuration of the buildings. Beams and columns were modeled as the elements with the plasticity concentrating over the specified hinge lengths at the element ends. This type of element is based on the non-iterative (or iterative) flexibility formulation. The elastic region that links the plastic ends only requires defining the element section area and the concrete elastic module. The hinge ends should be defined with a specific length  $L_p$  and a previously-defined fiber section. According to the studies by Panagiotakos and Fardis (2001), the hinge length is calculated by

$$L_p = 0.18L_s + 0.021a_{sl}d_b f_y \quad (4)$$

where  $L_s$  is the shear span of member;  $a_{sl}=1$  shows the effect of pullout of longitudinal bars is considered ( $a_{sl}=0$  is adopted here without considering this effect);  $d_b$  is the diameter of compressive bars; and  $f_y$  is the yield strength of tension reinforcement.

The fiber section consists of the layers of reinforcement bars and the patches of the unconfined cover concrete and the confined core concrete. A nonlinear constitutive material relationship with isotropic strain hardening (Menegotto and Pinto 1973) was adopted to define uniaxial nonlinear behavior of reinforcement bars. Six parameters are required to define the steel material, which are the initial stiffness  $E_s$ , the yield strength  $f_y$ , the ratio of the post yield to initial stiffness  $\alpha$ , and the parameters controlling the transition from the elastic to plastic branches,  $CR_1$ ,  $CR_2$  and  $R_0$ . Four steel parameters were taken as deterministic:  $CR_1=0.925$ ,  $CR_2=0.15$ ,  $R_0=20$ ,  $\alpha=0$ , while the left parameters, i.e.,  $E_s$  and  $f_y$ , were viewed as random (see section 4). The well-known nonlinear constitutive law by Kent and Park (1971) was used to define the uniaxial nonlinear behavior of concrete. This concrete material is determined by four parameters, i.e., the peak strength, the strain at peak strength, the residual strength, and the strain at which the residual strength is reached. For the unconfined concrete cover, these four parameters are termed as  $f_{cp,cover}$ ,  $\varepsilon_{cp,cover}$ ,  $f_{cu,cover}$  and  $\varepsilon_{cu,cover}$ , respectively, while they are denoted as  $f_{cp,core}$ ,  $\varepsilon_{cp,core}$ ,  $f_{cu,core}$  and  $\varepsilon_{cu,core}$  for the confined core concrete, respectively. During defining the core concrete parameters, the equations proposed by Scott *et al.* (1982) were employed to consider the additional confinement offered by the actual layouts, diameter and spacing of stirrups. Amongst the concrete parameters, only two were taken as deterministic:  $\varepsilon_{cp,cover}=0.002$  and  $f_{cu,cover}=0$ , while the left ones were viewed as uncertain (see section 4).

Fig. 8 summarizes the overall FE modeling contents. Rigid end zones were used for beam-column joint modeling. The columns of the first floor were modeled with a fixed base condition. Geometric nonlinearities have been incorporated in the form of P- $\Delta$  effects. Through FE linear analysis, the fundamental periods of the example frames are determined as 0.71 s, 0.90 s, 1.19 s and 1.47 s for the 3-, 5-, 8- and 10-story buildings, respectively, and the corresponding percentages of first modal mass are equal to 91%, 85%, 79% and 77%, respectively. It is clear that the 3- and 5-story buildings are first-mode dominant while the 8- and 10-story structures have a considerable sensitivity to the higher modes. Note that concrete cracking is not considered during determining the fundamental periods of the buildings. If it is considered, the calculated periods will be slightly increased.

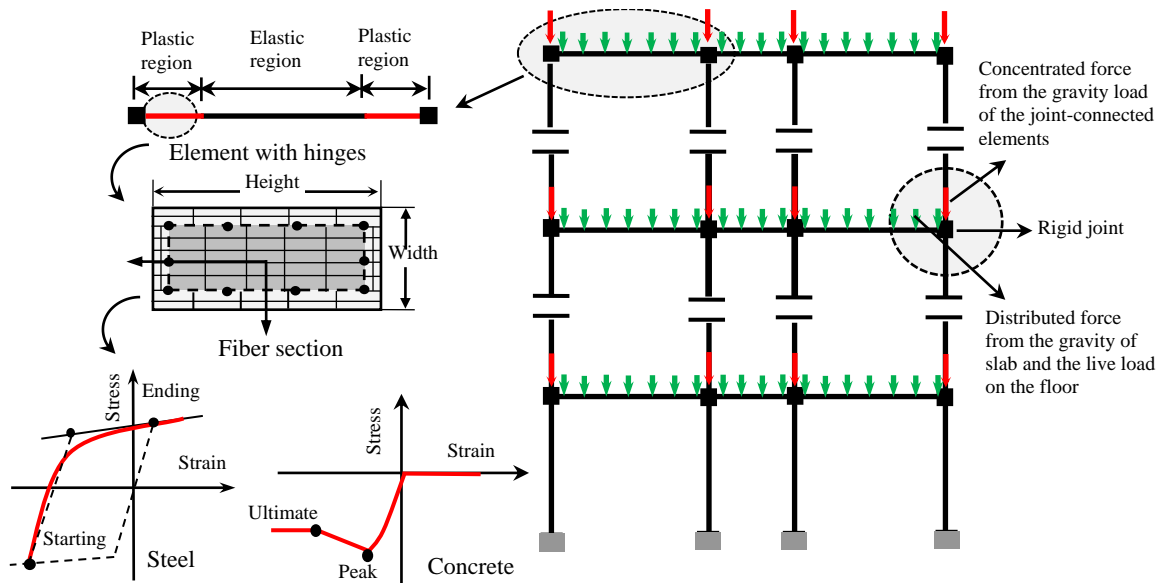


Fig. 8 Structural model on the OpenSees software platform

#### 4. Uncertainty parameters

A total of ten structural parameters are considered as random variables, involving the weight density of the reinforced concrete  $\rho_{\text{dead}}$ , the live load on the floor  $q_{\text{live}}$ , the yield strength  $f_y$  and the elastic modulus  $E_s$  of steel material, the peak strength  $f_{\text{cp,cover}}$  and the strain at the peak strength  $\epsilon_{\text{cp,cover}}$  of the cover concrete, and the peak strength  $f_{\text{cp,core}}$ , the strain at the peak strength  $\epsilon_{\text{cp,core}}$ , the residual strength  $f_{\text{cu,core}}$  and the strain at the residual strength  $\epsilon_{\text{cu,core}}$  of the core concrete. In these random variables,  $\rho_{\text{dead}}$  and  $q_{\text{live}}$  are assumed to follow a normal distribution and a Gamma distribution, respectively, and the remaining material parameters are lognormal variables. The

Table 2 Probabilistic distributions of the considered uncertainty parameters

Uncertainty source	Parameter	Mean	Coefficient of variation	Distribution type
Dead load	$\rho_{\text{Dead}}$	26.50 kN/m <sup>3</sup>	0.07	Normal
Live load	$q_{\text{Live}}$	0.98 kN/m	0.41	Gamma
	$f_{\text{cp,cover}}$	29.10 MPa	0.13	
	$\epsilon_{\text{cu,cover}}$	0.004	0.20	
	$f_{\text{cp,core}}$	37.95 MPa	0.20	
	$\epsilon_{\text{cp,core}}$	0.0021	0.16	
Concrete	$f_{\text{cu,core}}$	28.70 MPa	0.20	Lognormal
	$\epsilon_{\text{cu,core}}$	0.0110	0.52	
	$f_y$	378 MPa	0.07	
Reinforcing steel	$E_s$	200000 MPa	0.02	Lognormal

determination of the distribution parameters is not provided here but can be found in Lu *et al.* (2014). For reasons of completeness, the probabilistic distributions of the above random parameters are given in Table 2.

The correlation between the random parameters are considered according to Barbato *et al.* (2010):  $\rho=0.8$  for (i)  $f_{cp,cover}$  and  $f_{cp,core}$ ; (ii)  $f_{cp,core}$  and  $f_{cu,core}$ ; (iii)  $\varepsilon_{cu,cover}$  and  $\varepsilon_{cu,core}$ ; (iv)  $\varepsilon_{cp,core}$  and  $\varepsilon_{cu,core}$ ;  $\rho=0.64$  for (i)  $f_{cp,cover}$  and  $f_{cu,core}$ ; (ii)  $\varepsilon_{cu,cover}$  and  $\varepsilon_{cp,core}$ ; and  $\rho=0$  for all other pairs of parameters due to lack of knowledge. Note that the spatial variation of the random parameters within the structure is not considered here. All the random parameters are modeled as spatially fully correlated over the same structure.

## 5. Uncertainty analysis

### 5.1 Probabilistic pushover curves and the identified LS capacities

A displacement-controlled pushover procedure is adopted with incremental invariant lateral loads. Two lateral load patterns, namely the uniform load pattern and the SRSS load pattern, are used here to account for the effect of lateral forces on pushover responses. The uniform pattern applies the lateral forces that are proportional to the total mass at each floor level; while the SRSS pattern applies the lateral loads proportional to the story shears calculated by response spectrum analysis of the building to include sufficient modes to capture at least 90% of the total mass are used. The above choice of lateral load patterns is consistent with the suggestion by FEMA 273 (1997) that requires at least two vertical distributions of lateral loads, i.e., the uniform pattern and the model pattern, to be considered for nonlinear static analysis. The lateral forces used for pushover analysis is associated with the floor mass. Due to the uncertainty of the global load parameters as  $\rho_{dead}$  and  $q_{live}$ , the floor mass varies significantly, as shown in Fig. 9, where the 8-story frame is taken as the example. The variation of the lateral forces due to that in floor mass is accounted for in performing pushover analyses for random structural models.

Fig. 10 illustrates the pushover curves obtained from the random structural models when separately applying uniform and SRSS load patterns, where the LS thresholds are identified on

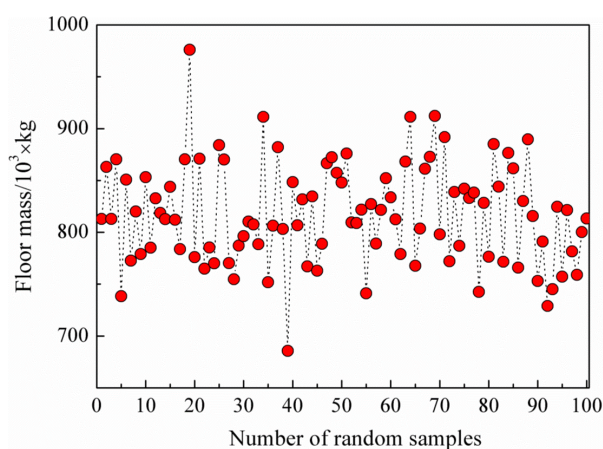


Fig. 9 Variation of floor mass due to the uncertainties in load parameters  $\rho_{dead}$  and  $q_{live}$

each curve according to the criteria listed in Table 1. Therein, the wide ranges of the pushover curves are apparent, illustrating the considerable effect of structural randomness on the capacity. The acquired LS capacities are shown in Fig. 11 for each considered LS. As seen from the figure, the thresholds corresponding to most of the concerned LSs scatter in a wide range. For instance, LS<sub>10</sub> has a wide drift scope that reaches  $0.5% < \theta_{max} < 6.0%$ . It is clear that merely using the deterministic threshold without considering the structural uncertainties will not provide the complete prediction of structural capacities, although the US standard (ASCE/SEI41-06 2007) and the Chinese code (GB50011 2010) support the use of arbitrary drift limits. It is also important to notice that the varieties of building designs and lateral load patterns also contribute to the wide drift scopes. These two factors in fact can only be incorporated in the simulation-based approach instead of the empirical code-provided thresholds. In other words, the empirical thresholds given in the codes are not suitable for the individual buildings if you want to know the real capacity.

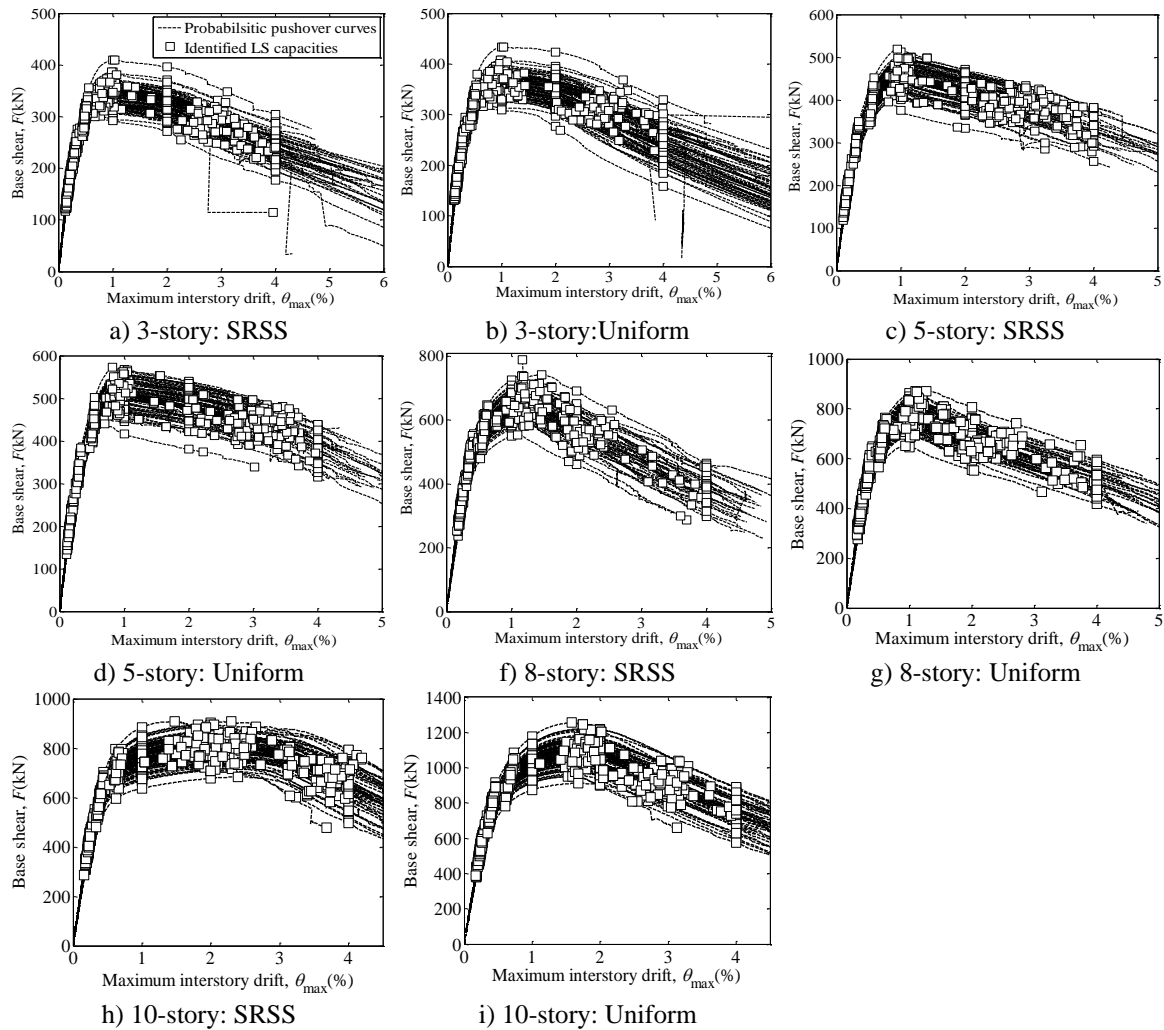


Fig. 10 Probabilistic pushover curves and the identified thresholds for the considered LSs

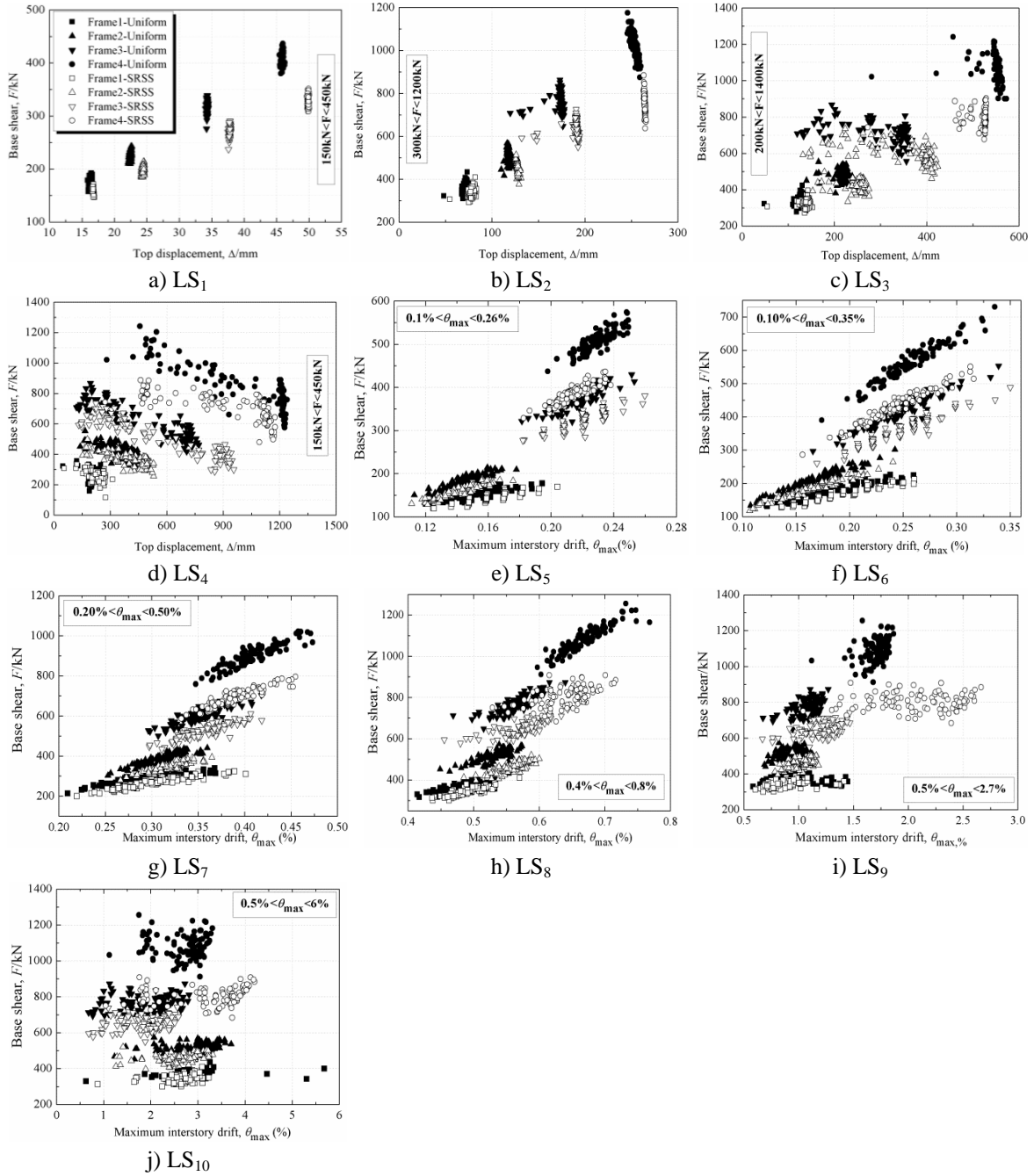


Fig. 11 Identified thresholds of the considered LSs from probabilistic pushover

5.2 Uncertainty analysis results:  $m_c$

Based on the obtained LS capacities, lognormal distributions are fitted for each considered LS

using the least-squares method and the corresponding parameters as  $m_C$  and  $\beta_C$  are derived. The influence of structural randomness on LS capacities is first examined by comparing  $m_C$  with the capacity  $C_m$  that is defined from the deterministic structural model using the median parameters. The difference between  $m_C$  and  $C_m$  is measured by

$$\alpha_{C,U} = \frac{|m_{C,U} - C_{m,U}|}{C_{m,U}} \tag{5}$$

and

$$\alpha_{C,S} = \frac{|m_{C,S} - C_{m,S}|}{C_{m,S}} \tag{6}$$

where  $\alpha_{C,U}$  and  $\alpha_{C,S}$  are the difference ratios calculated from the pushover responses when applying the uniform load pattern and the SRSS load pattern, respectively;  $m_{C,U}$  and  $m_{C,S}$  are the median capacities from the probabilistic pushover responses of the random structural models using the uniform load pattern and the SRSS load pattern, respectively; and  $C_{m,U}$  and  $C_{m,S}$  are defined from the deterministic pushover responses of the median structural models using the uniform load pattern and the SRSS load pattern, respectively.

The pushover responses from different lateral load patterns are then considered together, and the median capacity in terms of  $m_{C,T}$  is fitted. The mean value of  $C_{m,S}$  and  $C_{m,U}$  is used as the comparison and then the difference ratio  $\alpha_{C,T}$  is calculated by

$$\alpha_{C,T} = \frac{\left| m_{C,T} - \frac{(C_{m,S} + C_{m,U})}{2} \right|}{\frac{(C_{m,S} + C_{m,U})}{2}} \tag{7}$$

Table 3 Comparisons between  $m_C$  and  $C_m$  by  $\alpha_{C,U}$ ,  $\alpha_{C,S}$  and  $\alpha_{C,T}$

LS	3-story			5-story			8-story			10-story		
	$\alpha_{C,U}$	$\alpha_{C,S}$	$\alpha_{C,T}$									
LS <sub>1</sub>	0.42%	0.42%	1.19%	0.79%	0.78%	1.32%	0.18%	0.16%	1.06%	0.22%	0.07%	0.50%
LS <sub>2</sub>	0.61%	0.43%	1.18%	1.01%	0.92%	1.49%	1.33%	1.05%	1.38%	0.10%	0.39%	1.43%
LS <sub>3</sub>	2.38%	0.78%	2.15%	1.42%	0.80%	1.47%	2.72%	3.13%	3.01%	0.54%	0.83%	4.13%
LS <sub>4</sub>	1.21%	3.94%	2.75%	4.85%	2.83%	2.84%	24.54%	15.48%	19.38%	12.90%	10.04%	8.81%
LS <sub>5</sub>	1.00%	1.02%	0.61%	1.12%	1.09%	0.77%	1.01%	0.61%	0.73%	1.16%	0.76%	1.13%
LS <sub>6</sub>	2.57%	1.33%	2.17%	2.03%	1.42%	2.02%	1.32%	1.20%	0.91%	1.00%	0.59%	0.66%
LS <sub>7</sub>	0.33%	1.13%	0.93%	0.16%	0.23%	0.14%	1.44%	1.48%	1.68%	1.54%	0.85%	1.21%
LS <sub>8</sub>	0.01%	0.91%	0.41%	0.33%	0.76%	0.31%	3.03%	1.61%	1.95%	0.89%	0.10%	0.17%
LS <sub>9</sub>	4.40%	0.58%	2.18%	0.58%	0.71%	1.30%	1.01%	2.09%	3.85%	2.73%	1.30%	7.05%
LS <sub>10</sub>	2.60%	1.62%	1.88%	3.33%	2.27%	4.00%	10.32%	11.07%	11.14%	1.62%	6.21%	9.54%

Table 3 compares  $m_C$  and  $C_m$  for different LSs by  $\alpha_{C,U}$ ,  $\alpha_{C,S}$  and  $\alpha_{C,T}$ . It is found that the effect of structural uncertainties on the median capacities is actually negligible for the LSs other than that near collapse (LS<sub>4</sub> and LS<sub>10</sub>). For LS<sub>4</sub> ( $\theta_{\max}=4\%$ ) and LS<sub>10</sub> (20% reduced post-peak capacity), the corresponding median capacities are more sensitive to the variation of structural parameters than the other LSs. For instance, the difference ratio of  $\alpha_{C,T}$  is close to 20% for the 8-story frame while that of the 3- and 5-story frames are below 5%. This result implies that the building height also contributes to the variation of median capacities. Compared to the low-rise buildings (3- and 5-story), the mid-rise buildings (8- and 10-story) have larger difference ratios of median capacity at the LSs near collapse.

The LS capacities from different buildings and different lateral load patterns are considered together further. The overall difference ratio,  $\alpha_{C,TT}$ , is generated by

$$\alpha_{C,TT} = \frac{\left| m_{C,TT} - \frac{\sum_i^4 [C_{m,U}^i + C_{m,S}^i]}{8} \right|}{\frac{\sum_i^4 [C_{m,U}^i + C_{m,S}^i]}{8}} \quad (8)$$

where  $m_{C,TT}$  is fitted from the total thresholds for each considered LSs.

Fig. 12 shows the values of  $\alpha_{C,TT}$  calculated for different LSs. As revealed from this figure only the LSs near collapse, i.e., LS<sub>4</sub> and LS<sub>10</sub>, are significantly affected by structural uncertainties as the corresponding values of  $\alpha_{C,TT}$  greater than 10%. For the other LSs, LS<sub>9</sub> that is defined at the peak resistance and LS<sub>3</sub> that corresponds to the drift of 2% are moderately affected by structural uncertainties with the values of  $\alpha_{C,TT}$  between 5% and 10%, whereas the left LSs are total slightly affected by structural uncertainties showing the values of  $\alpha_{C,TT}$  below 2%. Merely based on the above observations we can conclude that structural uncertainties have not significant effects on the median capacities corresponding to the LSs except for that near collapse; therefore it is reasonable to determine  $m_C$  for these LSs using the code-provided or the deterministic pushover-based thresholds. However this simple treatment of  $m_C$  without considering the effects of structural uncertainties may cause the incorrect prediction on the median capacities for the LSs near collapse.

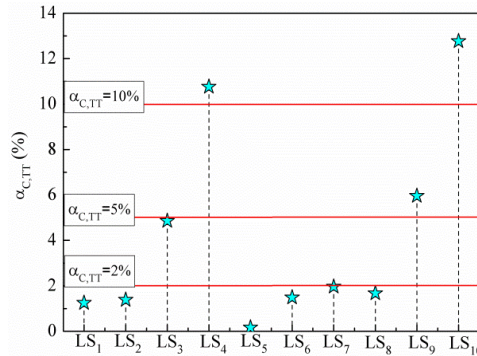


Fig. 12 Overall difference ratios of the median LS capacities

5.3 Uncertainty analysis results:  $\beta_C$

Let  $\beta_{C,U}$ ,  $\beta_{C,S}$  and  $\beta_{C,T}$  denote the dispersions of LS capacities from the pushover responses by the uniform load pattern, by the SRSS load pattern and by both of them, respectively. They are compared with the commonly used assumptions on the variation of LS capacities as  $\beta_C=0.25$  that was adopted by Ellingwood *et al.* (2007), and  $\beta_C=0.30$  that was recommended by Wen *et al.* (2004) and widely accepted by the following studies on seismic fragility assessment of RC buildings (Ramamoorthy *et al.* 2006, Hueste and Bai 2007). The comparison results are illustrated in Fig. 13. It is clear that the assumption of  $\beta_C$  between 0.25 and 0.30 is only suitable for describing the uncertainties associated with the LSs near collapse (LS<sub>4</sub> and LS<sub>10</sub>) for the 8- and 10-story frames, whereas it obviously overestimates the uncertainties in the other LSs. For instance, the dispersions with respect to LS<sub>1</sub>, LS<sub>2</sub>, LS<sub>3</sub>, LS<sub>5</sub> and LS<sub>8</sub> are even less than 0.1. For such a small uncertainty scale, if the assumption of  $\beta_C=0.30$  or  $\beta_C=0.25$  is still used, the resultant probabilistic capacity model will not be well predictable. Besides, no clear influence from building height is observed on the dispersion of LS capacities.

The overall dispersions in terms of  $\beta_{C,TT}$  are examined using the total LS capacities acquired from the pushover responses of different buildings with different lateral load patterns, as shown in Fig.14. Because the variation between different case buildings is additional involved, the derived dispersions of LS capacities are increased in comparison with that for the individual buildings. The

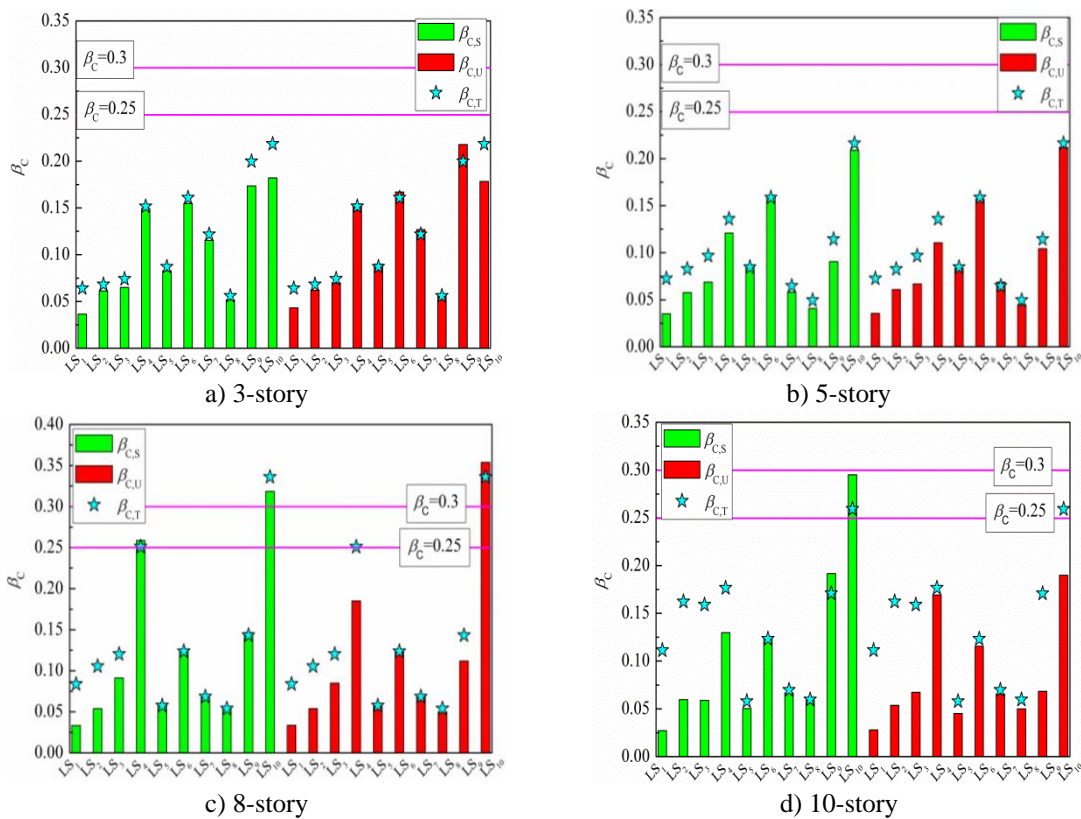


Fig. 13 Comparison of the calculated  $\beta_C$  with the that from empirical assumptions

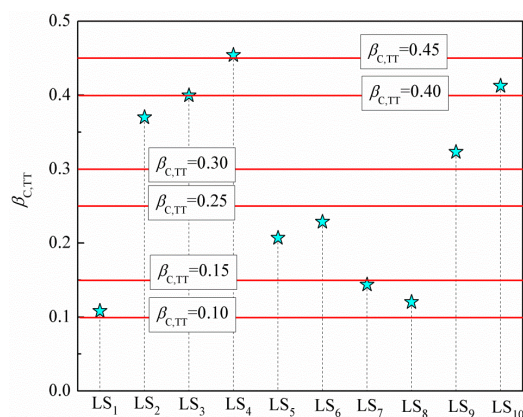


Fig. 14 The capacity dispersions of considered LSs from the pushover responses of the building group

capacity dispersions  $\beta_{C,TT}$  for the building group are beyond 0.30 even 0.40 at LS<sub>2</sub>, LS<sub>3</sub>, LS<sub>4</sub>, LS<sub>9</sub> and LS<sub>10</sub>. For LS<sub>5</sub> and LS<sub>6</sub>, the corresponding dispersions are beyond 0.20 while below 0.30, whereas the left LSs only show limited uncertainty with a value of  $\beta_{C,TT}$  around 0.10. Only from the above observations, the assumptions of  $\beta_C=0.25$  and  $\beta_C=0.30$  seems to be suitable for defining the uncertainties associated with moderate structural damages for the generic RC building group. But for the LSs near collapse (LS<sub>4</sub> and LS<sub>10</sub>) a larger  $\beta_C$  range between 0.40 and 0.45 seems proper and are suggested by this study. In addition, a rough approximation of  $\beta_C$  between 0.10 and 0.15 seems enough to consider the uncertainties with respect to these LSs related to slight damages.

## 6. Conclusions

The uncertainties in limit state (LS) capacities of RC frame buildings were assessed using a probabilistic pushover approach that adopted a correlation-controlled Latin hypercube sampling (CLHS) technique to determine the structural model set for accounting for the inherent randomness in structural parameters. Four typical RC frame buildings with 3, 5, 8 and 10 stories were used as the study cases. Ten of structural parameters including concrete and steel strengths and gravity loads were considered as random variables. Based on the CLHS, 100 structural models were derived for each case study frame and pushover analyses were repeatedly performed for each model. A set of ten LSs based on the design-code-given thresholds and the available damage-controlled criteria were acquired from the pushover responses of the random structural models. The obtained LS capacities were further fitted by the commonly used lognormal assumptions. The lognormal distribution parameters as the median capacity  $m_C$  and the logarithm standard deviation (dispersion)  $\beta_C$  were examined to extract the effect of structural uncertainties on LS capacities.

Based on the results of this study, structural randomness showed significant effect on the median capacities of the LSs close to collapse while the effects on the other LSs were negligible. Therefore it is reasonable to determine the median capacity  $m_C$  for the LSs far from collapse states with the thresholds provided by the design codes or the deterministic pushover analysis. However the structural uncertainties should be carefully considered when defining  $m_C$  for the LSs near

collapse. As for the dispersion  $\beta_C$  of LS capacities, the widely used assumption as  $\beta_C=0.25$  or  $0.30$  was found to overestimate the uncertainties in LS capacities for the individual buildings. However they seemed to be more suitable to describe the uncertainties associated with the LSs corresponding to moderate structural damages from the viewpoint of the building group. Also seen from the building group, a large scale of uncertainty as  $\beta_C=0.40\sim 0.45$  was suggested to be used for the LSs near collapse, and a relative small value of capacity dispersion between  $0.1$  and  $0.15$  seems adequate to describe the uncertainties inherent the LSs related to slight structural damages.

This study presented in this paper only uses four RC frame buildings as a case study with the aim to provide a quantitative assessment of the uncertainties in LS capacities of structures by considering the randomness in structural parameters. Due to the limitation of the study cases, the above findings may differ with varying building properties, uncertain parameters, response parameters and the used criteria to identify limit states on a pushover curve. However the methodology presented in this paper is general in scope and it is beneficial to estimate the uncertainties in LS capacities especially for the individual buildings. Moreover, the problem of uncertainty treatment in LS capacities is a common theme in seismic fragility and risk assessment of structural portfolios. The obtained findings here help develop reliable fragility curves for different types of structures for use in seismic risk assessments.

## Acknowledgements

The financial support received from the Scientific Research Foundation for the Returned Overseas Chinese Scholars, State Education Ministry, the National Science Foundation of China (Grant Nos. 51408155, 51378162), the China Postdoctoral Science Foundation (2014M551251), the Heilongjiang Postdoctoral Science Foundation (LBH-Z14114), and the Fundamental Research Funds for the Central Universities (HIT. NSRIF. 2015099) are gratefully appreciated.

## References

- ATC 40 (1996), *Seismic evaluation and retrofit of concrete buildings: volume 1*, Applied Technology Council, State of California, seismic safety commission, USA.
- ASCE/SEI41-06 (2007), *Seismic Rehabilitation of Existing Buildings*, American Society of Civil Engineers, Reston, Virginia, USA.
- Barbato, M., Gu, Q. and Conte, J.P. (2010), "Probabilistic Push-Over analysis of structural and soil-structure systems", *J. Struct. Eng.*, ASCE, **136**(11), 1330-1341.
- Celik, O.C. and Ellingwood, B.R. (2010), "Seismic fragilities for non-ductile reinforced concrete frames - Role of aleatoric and epistemic uncertainties", *Struct. Saf.*, **32**(1), 1-12.
- Choe, D.E., Gardoni, P. and Rosowsky, D. (2007), "Closed-form fragility estimates, parameter sensitivity, and Bayesian updating for RC columns", *J. Eng. Mech.*, ASCE, **133**(7), 833-843.
- Cornell, C.A., Jalayer, F., Hamburger, R.O. and Foutch, D.A. (2002), "Probabilistic basis for 2000 SAC federal emergency management agency steel moment frame guidelines", *J. Struct. Eng.*, **128**(4), 526-533.
- Dolšek, M. (2009), "Incremental dynamic analysis with consideration of modeling uncertainties", *Earthq. Eng. Struct. Dyn.*, **38**(6), 805-825.
- Dolšek, M. (2012), "Simplified method for seismic risk assessment of buildings with consideration of aleatory and epistemic uncertainty", *Struct. Infrastruct. Eng.*, **8**(10), 939-953.
- Ellingwood, B.R., Celik, O.C. and Kinali, K. (2007), "Fragility assessment of building structural systems in

- Mid-America”, *Earthq. Eng. Struct. Dyn.*, **36**(13), 1935-1952.
- Erberik, M.A. and Elnashai, A.S. (2004), “Fragility Analysis of Flat-slab Structures”, *Eng. Struct.*, **26**(7), 937-948.
- Erberik, M.A. (2008), “Generation of fragility curves for Turkish Masonry buildings considering in-plane failure modes”, *Earthq. Eng. Struct. Dyn.*, **37**(3), 387-405.
- Favvata, M.J., Naoum, M.C. and Karayannis, C.G. (2013), “Limit states of RC structures with first floor irregularities”, *Struct. Eng. Mech.*, **47**(6), 791-818.
- FEMA 273 (1997), *NEHRP guidelines for the seismic rehabilitation of buildings*, Federal Emergency Management Agency, Washington DC, USA.
- FEMA (1999), *HAZUS earthquakes loss estimation methodology*, Federal Emergency Management Agency, Washington DC, USA.
- Frankie, T.M., Gencturk, B. and Elnashai, A.S. (2013), “Simulation-Based fragility relationships for unreinforced Masonry buildings”, *J. Struct. Eng.*, ASCE, **139**(3), 400-410.
- Gardoni, P., Der Kiureghian, A. and Mosalam, K.M. (2002), “Probabilistic capacity models and fragility estimates for reinforced concrete columns based on experimental observations”, *J. Eng. Mech.*, ASCE, **128**(10), 1024-1038.
- GB50010 (2010), *Code for Design of Concrete Structures*, National Standards of the People’s Republic of China, Beijing.
- GB50011 (2010), *Code for Seismic Design of Buildings*, National Standards of the People’s Republic of China, Beijing.
- Howary, H.A.E. and Mehanny, S.S.F. (2011), “Seismic vulnerability evaluation of RC moment frame buildings in moderate seismic zones”, *Earthq. Eng. Struct. Dyn.*, **40**(2), 215-235.
- Hueste, M.B.D. and Bai, J.W. (2007), “Seismic retrofit of a reinforced concrete flat-slab structure: Part II-seismic fragility analysis”, *Eng. Struct.*, **29**(6), 1178-1188.
- Ji, J., Elnashai, A.S. and Kuchma, D.A. (2007), “Seismic fragility relationships of reinforced concrete high-rise buildings”, *Struct. Des. Tall Spec. Build.*, **18**(3), 259-277.
- Kent, D.C. and Park, R. (1971), “Flexural members with confined concrete”, *J. Struct. Div.*, ASCE, **97**(7), 1969-1990.
- Kwon, O.S. and Elnashai, A.S. (2006), “The effect of material and ground motion uncertainty on the seismic vulnerability curves of RC structure”, *Eng. Struct.*, **28**(2), 289-303.
- Lu, D.G., Yu, X.H., Jia, M.M. and Wang, G.Y. (2014), “Seismic risk assessment of a RC frame designed according to Chinese codes”, *Struct. Infrastruct. Eng.*, **10**(10), 1295-1310.
- Menegotto, M. and Pinto, P.E. (1973), “Method of analysis for cyclically loaded RC plane frames including changes in geometry and non-elastic behaviour of elements under combined normal force and bending”, *Proceedings of IABSE Symposium on Resistance and Ultimate Deformability of Structures Acted on by Well Defined Repeated Loads*, Lisbon, Portugal.
- Mwafy, A. (2012), “Analytically derived fragility relationships for the modern high-rise buildings in the UAE”, *Struct. Des. Tall. Spec. Build.*, **21**(11), 824-843.
- Olsson, A.M.J. and Sandberg, G.E. (2002), “Latin hypercube sampling for stochastic finite element analysis”, *J. Eng. Mech.*, **128**(1), 121-125.
- OpenSees (2012), *Open system for earthquake engineering simulation*, Pacific Earthquake Engineering Research Center, University of California, Berkeley, CA.
- Ozel, A.E. and Guneyisi, E.M. (2011), “Effects of eccentric steel bracing systems on seismic fragility curves of mid-rise RC buildings - A case study”, *Struct. Saf.*, **33**(1), 82-95.
- Park, R. (1988), “Ductility evaluation from laboratory and analytical testing”, *Proceedings of the 9th World Conference on Earthquake Engineering*, Vol. VIII, Japan Association for Earthquake Disaster Prevention, Tokyo-Kyoto, Japan.
- Pasticier, L., Claudio, A. and Fragiaco, M. (2008), “Non-linear seismic analysis and vulnerability evaluation of a Masonry building by means of the SAP2000 V.10 code”, *Earthq. Eng. Struct. Dyn.*, **37**(3), 467-485.
- Panagiotakos, T.B. and Fardis, M.N. (2001), “Deformations of reinforced concrete members at yielding and

- ultimate”, *ACI Struct. J.*, **98**(2), 135-148.
- Ramamoorthy, S.K., Gardoni, P. and Bracci, J.M. (2006), “Probabilistic demand models and fragility curves for reinforced concrete frames”, *J. Struct. Eng.*, ASCE, **132**(10), 1563-1572.
- Rota, M., Penna, A. and Magenes, G. (2010), “A methodology for deriving analytical fragility curves for masonry buildings based on stochastic nonlinear analysis”, *Eng. Struct.*, **32**(5), 1312-1323.
- Shome, N. and Paolo, B. (2010), “Comparison of vulnerability of a new high-rise concrete moment frame structure using HAZUS and nonlinear dynamic analysis”, *Proceedings of the 10th international conference on structural safety and reliability (ICOSSAR 2009)*, Osaka, Japan.
- Scott, B.D., Park, P. and Priestley, M.J.N. (1982), “Stress-strain behavior of concrete confined by overlapping hoops at low and high-strain rates”, *ACI Struct. J.*, **79**(1), 13-27.
- Tomos, G.C. and Trezos, C.G. (2006), “Examination of the probabilistic response of reinforced concrete structures under static non-linear analysis”, *Eng. Struct.*, **28**(1), 120-133.
- Tran, C.T.N. and Li, B. (2014), “Experimental studies on the backbone curves of reinforced concrete columns with light transverse reinforcement”, *J. Perform. Constr. Facil.*, **29**(5), 04014126.
- Tran, C.T.N. and Li, B. (2013), “Ultimate displacement of reinforced concrete columns with light transverse reinforcement”, *J. Earthq. Eng.*, **17**(2), 282-300.
- Vamvatsikos, D. and Fragiadakis, M. (2010), “Incremental dynamic analysis for estimating seismic performance sensitivity and uncertainty”, *Earthq. Eng. Struct. Dyn.*, **39**(2), 141-163.
- Wen, Y.K., Ellingwood, B.R. and Bracci, J.M. (2004), *Vulnerability function framework for consequence-based engineering*, Technical Report No. DS-4, Mid-America Earthquake Center (MAE), University of Illinois at Urbana-Champaign, USA.
- Zhang, W. and Goh, A.T.C. (2014), “Multivariate adaptive regression splines model for reliability assessment of serviceability limit state of twin caverns”, *Geomech. Eng.*, **7**(4), 431-458.